JOURNAL OF GUIDANCE, CONTROL, AND DYNAMICS
Vol. 23, No. 1, January–February 2000

Mode Localization in Flexible Spacecraft: A Control Challenge

Robert E. Zee* and Peter C. Hughes†
University of Toronto, Toronto, Ontario, M3H 5T6, Canada

Mode localization is often an unexpected phenomenon in flexible space structures because it arises from very small manufacturing errors. It will occur, however, in structures comprising lightly damped, weakly coupled repeating members that have tightly clustered modes of vibration. If not properly taken into account, mode localization can potentially pose problems for high-performance flexible spacecraft controllers relying on the assumption of perfect symmetry. In cases where actuation and sensing are limited, local decentralized control design for each structural member relies on the propagation of energy from one member to the next through channels of weak coupling. Mode localization can severely inhibit this propagation leading to control performance degradation. A solution to this problem is to design controllers based on models consisting of multiple members of the structure or to centralize control design. Because mode shape errors can be large when modes localize, however, any uncertainty model that attempts to capture this information will lead to reduced control authority, overconservatism, and performance losses. It is shown that eigenvalue perturbation models are an effective means by which to design controllers for flexible space structures subject to mode localization. The successful control of a structure with mode localization is demonstrated through experiments conducted on a flexible spacecraft emulator that exhibits the phenomenon.

Nomenclature

$\mathcal{B}$ = input distribution matrix
$\mathcal{C}$ = output distribution matrix
$\mathcal{D}$ = damping matrix
$\mathcal{E}$ = matrix of natural mode shapes
f = column matrix of generalized forces
$\mathcal{K}$ = stiffness matrix
$\mathcal{M}$ = mass matrix
q = column matrix of physical coordinates (displacements)
T_a = actuator dynamics
W_{w1} = input disturbance weight
W_{w2} = sensor noise weight
W_{z1} = system coordinate weight
W_{z2} = control force weight
w_1 = input disturbances
w_2 = sensor noise
y = column matrix of measurements
z_1 = weighted system coordinates
z_2 = weighted control forces
η = column matrix of modal coordinates
Ψ = diagonal matrix of damping factors
Ω = diagonal matrix of natural frequencies

Introduction

IN physical systems comprising weakly coupled repeating members, slight departures from perfect regularity may result in significant modal distortion and impede the propagation of vibrational energy. This phenomenon, known as mode localization, was originally studied in the field of solid-state physics by Anderson,[1] who predicted the effect of defects on lattice vibrations. On a more macroscopic level, the phenomenon is relevant to flexible space structures (FSS) that possess the requirements for localization: weak coupling, spatial periodicity, and the attendant clustering of natural frequencies. Mode localization is the process by which the spatial extent of a natural mode localizes to a single or limited number of structural members.

When modes localize, disturbances tend to confine themselves to the regions of the structure from which they originated. If those regions are unactuated or unsensed, relying on the free propagation of vibrations to other, well-controlled parts of the structure proves ineffectual. Even when this is not the case, the presence of slight structural asymmetries can complicate control design by generating large modal errors relative to an assumed model. The end result is an overly conservative control design at best and an unstable one at worst. As coupling between members drops, the sensitivity to asymmetry increases, as does the propensity of modes to localize. For structures with very weak coupling, modes could localize even for the slightest departure from perfect regularity.

In FSS, the degree to which modes localize is dependent on the ratio of imperfection (asymmetry) to the strength of coupling between structural members. Coupling strength is indicated by the extent to which natural frequencies are clustered together. Imperfection is a measure of how different structural members are from their nominal properties. The transition from the modes of a symmetric structure to localized modes is not abrupt, but smooth and continuous.[2] Because mode localization is dependent not only on the amount of asymmetry, but also on coupling strength, there is no hard number for imperfection that determines the degree of localization. For FSS, coupling is typically such that severe localization (mode shapes confined mainly to one structural member) is induced by less than a 5% stiffness variation between structural members.

Theoretical investigations of mode localization have been conducted on one-dimensional structures such as coupled pendula swinging in a plane and truss structures, both of which can be modeled as mass–spring systems.[3–6] Because closed-form analysis becomes difficult for all but one-dimensional structures, two-dimensional structures have been studied both numerically by Bendiksen[7] and Cornwell and Bendiksen[8] and experimentally by Levine-West and Salama.[9] These latter numerical and experimental studies are of greater relevance to the discussion at hand given the similarities shared between their ribbed antennas and the Daisy facility at the University of Toronto.

Research in the field to date has focused on demonstrating mode localization in structures and characterizing its nature. Various methods for expressing the amount of localization have been suggested. The impact of this phenomenon on system identification and control has yet to be explored, but it is hypothesized that mode localization can reduce the effectiveness of strategies that are based on symmetry. Mester and Benaroya,[6] Bendiksen,[7] Cornwell and Bendiksen,[8]

Received 10 June 1998; revision received 20 July 1999; accepted for publication 20 July 1999.

*Manager, Space Flight Laboratory, Institute for Aerospace Studies, 4925 Dufferin Street. Member AIAA.

†Professor, Institute for Aerospace Studies, 4925 Dufferin Street. Associate Fellow AIAA.

and Levine-West and Salama[9] all suggest that mode localization can present a problem for control strategies that are based on the assumption of perfect structural symmetry.

Nevertheless, some features of mode localization may be of benefit if mission-critical parts of a flexible spacecraft remain isolated from less critical, disturbed parts. Shelley and Clark[10] have examined the possibility of inducing mode localization through active control. Their analysis, however, does not address the issue when mode localization is a source of uncertainty for control. To the knowledge of the authors, no direct investigation into the control of FSS with localized modes has been reported. Yet, a surprising number of flexible spacecraft exhibit the characteristics that render them susceptible to this phenomenon.

It is not sufficient to say that, for control, models in physical coordinates should be used instead of models in modal coordinates. Structures with continuous flexibility tend to have myriad physical coordinates courtesy of finite element analysis. Only in modal coordinates can the most important dynamics of the system be captured through a low-order model.

It is also not sufficient simply to say that imperfections can be measured accurately on the ground before on-orbit operation. Although mass properties are relatively easy to measure, precise stiffness and damping properties remain elusive. The limitations of ground-based tests also contribute to this uncertainty.[11] On-orbit system identification could help remedy the situation, although it may not remove all uncertainty associated with localization given the very small structural imperfections needed to cause it. Moreover, system identification techniques might themselves be hindered by mode localization. Given the weak coupling inherent in FSS and that slight unaccounted for asymmetries are inevitably present in these structures, mode localization presents a real, practical problem. (Intentionally making the structure very asymmetric may eliminate the problem, but this strategy might itself face economic or mission-specific opposition.)

The present contribution is to demonstrate the successful control of a structure with localized modes using experiments at the Daisy facility. Specifically, the utility of eigenvalue perturbation models is illustrated in designing controllers for FSS subject to mode localization. The goal here is not to elaborate on the plenitude of mode localization analyses, nor is it to present new control theory. The objectives are 1) to show that modern control techniques, if used appropriately, are suited to handle the mode localization problem and 2) to apply them to a structure with mode localization.

In the sequel, structures with mode localization (ML) are referred to as ML structures, with apologies to the medical professional for treating the phenomenon as if it were a disease.

Localized Modes of Daisy

To better understand ML, we describe the Daisy facility a ground-based FSS emulator that exhibits the phenomenon and that is used to conduct the laboratory study.

Daisy emulates the behavior of FSS. It has lightly damped modes that cluster together at low frequencies in addition to rigid rotational freedom. The structure consists of 10 ribs mounted in a conical fashion atop a rigid hub (see Fig. 1). Each rib is attached to the hub by a universal joint that allows it to swing up and down and from side to side. These two types of rotation are referred to as out-of-cone and in-cone motion, respectively. Coupled to their neighbors by weak springs, the ribs also have stiffness relative to the hub in both rotational directions. For convenience, ribs are numbered in a clockwise fashion from above. The hub rotates about three axes afforded by a large universal joint and an air bearing. Two of the three axes are slightly pendulous from the effect of gravity.

In terms of actuation, each rib is controlled by lateral and vertical air thrusters that alter the shape of the cone formed by the ribs. The hub also houses three reaction wheels that impart control torques to Daisy, affecting its attitude. Rib configuration is determined via an optical sensing system, whereas hub orientation is measured by position encoders.

The internal structural dynamics of Daisy's components can be ignored compared to the slow macroscopic motions of the hub and ribs relative to one another. Thus, Daisy is said to have discrete flexibility because each rib has only two degrees of freedom relative to the hub. Other flexible space structures, however, may possess continuous flexibility, where structural members have a large number of flexible degrees of freedom. These in turn lead to a theoretically large number of structural modes, of which only the first several may be significant. Daisy's dynamics, therefore, adequately represent the dynamics of a FSS with continuous flexibility truncated to the most significant modes of vibration. Furthermore, the discrete nature of Daisy flexibility makes the present analysis more manageable, although results can easily generalize to cases of higher-dimensional flexibility.

Table 1 Empirically observed natural frequencies for Daisy ribs

Rib	OC frequency, Hz	% from nominal	IC frequency, Hz	% from nominal
1	0.083	−9	0.125	7
2	0.089	−3	0.115	−1
3	0.092	1	0.120	3
4	0.082	−10	0.115	−1
5	0.089	−3	0.119	2
6	0.110	20	0.097	−17
7	0.089	−3	0.117	1
8	0.096	5	0.128	10
9	0.082	−10	0.121	4
10	0.115	26	0.125	7

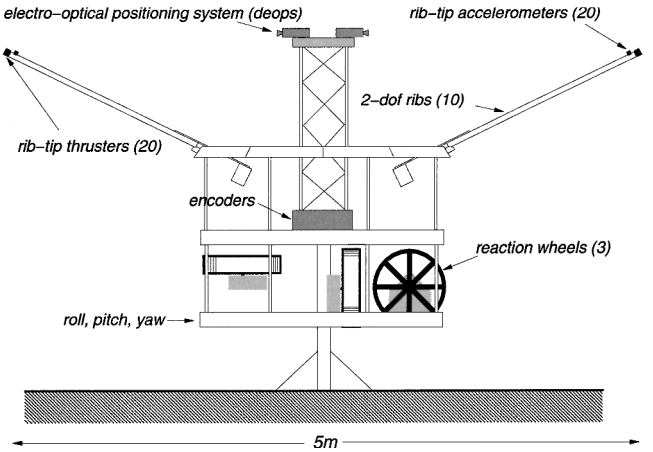

Fig. 1 Daisy facility. For simplicity, only 2 out of 10 ribs are shown.

As shown by Zee,[12] ML is a phenomenon that is associated only with purely flexible modes of vibration. For this reason, it is sufficient to study only the flexible subsystem of Daisy and to lock the hub in place. In the present analysis, therefore, only the flexible dynamics of Daisy are considered.

The natural modes of Daisy cluster in two groups: the out-of-cone modes and the in-cone modes. Obviously, these two mode groups arise from two types of rib motion. Nominally, the out-of-cone frequency of a single rib is about 0.091 Hz, whereas the in-cone frequency is around 0.116 Hz. Because coupling is weak, especially in the out-of-cone direction, the resulting modes of the entire system cluster around these two frequencies (10 modes each). Empirically observed modal damping is around 2–3%. If all ribs were identical and possessed the same nominal properties, frequency clustering would be accompanied by mode shapes with global rib participation. Under a 1% variation of stiffness between neighboring ribs, as a direct result of weak coupling in the out-of-cone direction, the out-of-cone modes localize to individual ribs as shown in Fig. 2. ML also results in a spreading of natural frequencies within each mode group.

Table 1 summarizes the empirically observed natural frequencies of each rib and their percent differences from nominal. The out-of-cone frequencies differ from nominal by 1–26%, whereas the in-cone frequencies vary by 1–17%. Given approximate knowledge of the coupling stiffness between ribs, the mathematical model of Daisy predicts that the differences between neighboring ribs are enough

Table 2 Modal frequencies and length scales (observed damping is around 2–3%)

Mode	Ideal frequency, Hz	Observed frequency, Hz	Normalized length scale	Dominant rib(s)
1	0.0915	0.0825	0.10	4 (OC)
2	0.0916	0.0825	0.15	9 (OC)
3	0.0916	0.0837	0.15	1 (OC)
4	0.0916	0.0888	0.30	5, 7 (OC)
5	0.0916	0.0889	0.16	2 (OC)
6	0.0918	0.0889	0.31	5, 7 (OC)
7	0.0918	0.0924	0.15	3 (OC)
8	0.0920	0.0962	0.15	8 (OC)
9	0.0920	0.108	0.24	6 (IC)
10	0.0922	0.110	0.10	6 (OC)
11	0.116	0.115	0.10	10 (OC)
12	0.119	0.120	0.59	2–4 (IC)
13	0.119	0.124	1.08	1, 2, 4, 5, 7–10 (IC)
14	0.127	0.127	0.84	9 (IC)
15	0.127	0.130	0.60	7 (IC)
16	0.135	0.136	0.84	3 (IC)
17	0.135	0.138	0.96	5 (IC)
18	0.141	0.143	0.69	3–5 (IC)
19	0.141	0.146	0.63	1, 8 (IC)
20	0.144	0.149	0.45	8–10 (IC)

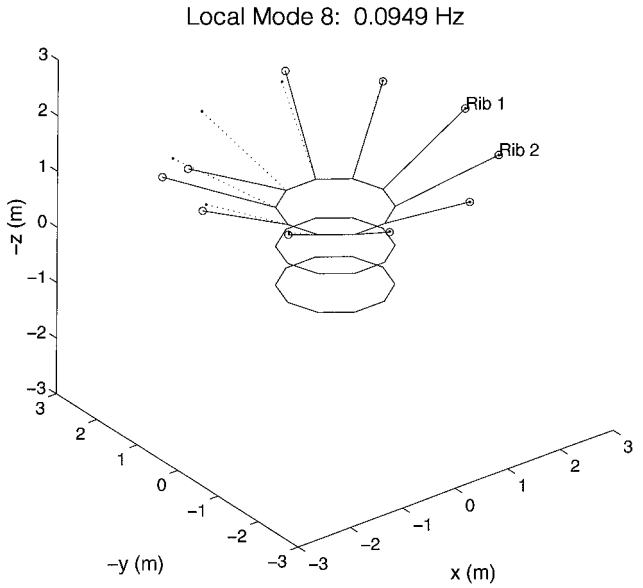

Fig. 2 ML phenomenon.

to cause severe localization among the out-of-cone modes and mild to severe localization among the in-cone modes. Space limitations prevent a complete illustration of modes, but terminology can be explained with reference to Fig. 2. Severe refers to the localization of a mode almost entirely to one rib (Fig. 2), whereas mild refers to the case where a mode shape is asymmetric and one rib participates slightly more than the others.

Cornwell and Bendiksen[2] propose a normalized length scale as a quantitative measure of the degree to which a mode is localized. Table 2 summarizes the normalized length scales for Daisy's natural modes, together with the vibration frequencies for both the perfectly symmetric and actual cases. The normalized length scale is related to the number of participating ribs in a mode, as compared to its counterpart in the perfect structure. It may be thought of as the approximate fraction of the number ribs participating in the asymmetric structure compared to the number participating in the perfect structure. The lower is the value, the greater is the severity of localization. For Daisy, the lowest possible value is 0.1. A value of unity indicates no deviation from the perfect structure.

The frequencies for the nominal perfectly symmetric structure are provided for comparison in Table 2. The corresponding ideal mode shapes have spatial distributions that vary sinusoidally with rib number. From lowest to highest frequency, the first perfect out-of-cone mode (mode 1) has a spatial period of two ribs, whereas the last (mode 10) is an umbrella mode. Spatial periodicity is reversed for the in-cone modes (modes 11–20). Mode localization changes these modes by restricting them to a single or reduced number of ribs.

In the analysis of Daisy, the authors are fortunate (for the purposes of conducting this research) to have a structure with properties that, in general, depart significantly from the nominal ones assumed on paper. Precise measurements are not needed to determine how strongly modes localize. For real FSS, however, the perturbations could be so small that they cannot be easily measured and yet produce localization.

The problem of localization in Daisy may be even worse considering actuator and sensor misalignments. Zee[12] has shown that these errors have an equivalent input–output interpretation in terms of mode-shape errors. The misalignment of the ribs themselves are responsible in part for the localization described in Table 2. In a study performed by Hong,[13] it is shown that imperfections in Daisy can be significantly large. From the evidence, Daisy is a ML structure that is ideal for the study at hand.

Problem for Control Design

ML presents a problem for control based on two observations.

1) Localization results in the confinement of disturbance energy to the point of excitation. Free vibrations travel only with great difficulty, even over long periods of time.

2) Localized mode shapes are dramatically different from the mode shapes of the perfectly symmetric structure assumed on paper. Accompanying this is the attendant spreading of previously clustered natural frequencies. Depending on how they are modeled, uncertainties may be large enough to affect the performance of centralized controllers.

The easiest way to control any flexible structure is to directly sense and actuate all critical coordinates. When enough sensors and actuators are available and coupling is weak, the input to a structural member primarily depends on the movement of that member. This is known as decentralized control and arises whether separate controllers are designed for each member (decentralized design) or a single controller is designed for the entire system (centralized design). Decentralized control has been shown to have a natural immunity to ML and modal errors.[12] This is the best scenario the control engineer could hope for.

Ideal situations are rare, however, and often the control engineer must be content with a reduced set of sensors and actuators. Independent decentralized control design for each structural member is dangerous in this case, especially for structures susceptible to ML. Relying on the propagation of energy through channels of weak coupling is futile for structures that are strongly localized. Under these circumstances, the only hope is that unactuated and unsensed parts of the structure are damped heavily enough, so that confined disturbance energy dissipates quickly.

Limited actuation and sensing schemes necessitate centralized control design leading to centralized control. In this way, the interaction between structural members, albeit weak, permits the movement of one member to actively damp the motions of another. The drawback with this approach lies in its sensitivity to system modal errors and to ML. The ability to model uncertainty effectively in this case is critical to avoiding overconservatism and excessive performance losses.

It is shown in the next section that the large mode-shape errors that characterize ML structures can be eliminated by a change of state. This effectively shifts the uncertainty to eigenvalues or natural frequencies and damping factors. Thus, eigenvalue perturbation models, as discussed by Smith,[14] can be applied to the ML problem. Control formulations based solely on frequency and damping uncertainty have been shown to produce excellent results by Smith et al.[15] and Balas and Young.[16] In their work, however, it is not explicitly stated how mode-shape errors are taken into account, although it is hinted that resulting controllers are robust to all model errors within the control bandwidth. Moreover, Balas and Young limit their perturbations to being diagonal (or parametric), whereas a change of state is more consistent with the unstructured approach

of Smith.[14] For the ML problem, however, mode-shape errors can be the most dominant, and most difficult, aspect to model and so deserve a more direct treatment. Eliminating mode-shape uncertainty has the effect of raising control authority, which in turn permits better performance. This is why eigenvalue perturbation models have demonstrated superior results over additive and multiplicative uncertainty models and are ideally suited for the ML control problem.

Shifting eigenvector errors to eigenvalue perturbations through a change of state can be done with any uncertainty formulation based on modal errors. A simple unstructured uncertainty approach is presented to demonstrate the value of eigenvalue perturbation models in the control of a FSS emulator that exhibits ML. Eigenvalue perturbation concepts are not limited to a single uncertainty formulation, but may be applied to any that use modal information.

The goal of the present study is to unite two worlds: ML and control. It deals with the application of modern control theory to solve an unaddressed problem. Experiments in the Daisy facility demonstrate that effective control is possible for ML structures using eigenvalue perturbation models.

Practical Solution

Eigenvalue perturbation concepts can be applied to any formulation that uses modal information. The utility of eigenvalue perturbation models for ML-afflicted structures is now demonstrated through a simple control formulation. The solution to the ML control problem is to carry modal errors entirely by eigenvalue perturbations through a change of state. Eliminating mode-shape errors, especially the large ones found in ML structures, removes any unnecessary restrictions on control authority, reduces overconservatism, and improves control performance.

The structure under control can be represented by the linear physical model

$$\mathcal{M}\ddot{\boldsymbol{q}} + \mathcal{D}\dot{\boldsymbol{q}} + \mathcal{K}\boldsymbol{q} = \mathcal{B}\boldsymbol{f} \tag{1}$$

$$\boldsymbol{y} = \mathcal{C}\boldsymbol{q} \tag{2}$$

Let $\mathcal{E}$ be the matrix of natural mode shapes for Eq. (1), so that $\mathcal{E}^T\mathcal{M}\mathcal{E}=\mathbf{1}$ (identity). By using the substitution $\boldsymbol{q}=\mathcal{E}\eta$ and rewriting Eq. (1) in first-order form, we have

$$\begin{bmatrix}\dot{\eta}\\ \ddot{\eta}\end{bmatrix} = \begin{bmatrix}\mathbf{0} & \mathbf{1}\\ -\boldsymbol{\Omega}^2 & -2\boldsymbol{\Psi}\end{bmatrix}\begin{bmatrix}\eta\\ \dot{\eta}\end{bmatrix} + \begin{bmatrix}\mathbf{0}\\ \mathcal{E}^T\mathcal{B}\end{bmatrix}f \tag{3}$$

$$\boldsymbol{y} = [\mathcal{C}\mathcal{E}\quad \mathbf{0}]\begin{bmatrix}\eta\\ \dot{\eta}\end{bmatrix} \tag{4}$$

This is the nominal model of the system. In general, the actual system is different and is given by

$$\begin{bmatrix}\dot{\eta}_p\\ \ddot{\eta}_p\end{bmatrix} = \begin{bmatrix}\mathbf{0} & \mathbf{1}\\ -\boldsymbol{\Omega}_p^2 & -2\boldsymbol{\Psi}_p\end{bmatrix}\begin{bmatrix}\eta_p\\ \dot{\eta}_p\end{bmatrix} + \begin{bmatrix}\mathbf{0}\\ \mathcal{E}_p^T\mathcal{B}\end{bmatrix}f \tag{5}$$

$$\boldsymbol{y} = [\mathcal{C}\mathcal{E}_p\quad \mathbf{0}]\begin{bmatrix}\eta_p\\ \dot{\eta}_p\end{bmatrix} \tag{6}$$

The p subscripts indicate that the actual system is perturbed away from the nominal model.

The additive perturbations to the nominal model that are needed to represent the system accurately are

$$\boldsymbol{D}\mathcal{E} = \mathcal{E}_p - \mathcal{E} \qquad \boldsymbol{D}\boldsymbol{\Omega}^2 = \boldsymbol{\Omega}_p^2 - \boldsymbol{\Omega}^2 \qquad \boldsymbol{D}\boldsymbol{\Psi} = \boldsymbol{\Psi}_p - \boldsymbol{\Psi} \tag{7}$$

For structures that suffer from ML, the entries in $\boldsymbol{D}\mathcal{E}$ can be just as large as the entries in $\mathcal{E}$, rendering the modal matrix highly uncertain. If anticipated errors are modeled in this way, by considering matrices such as $\boldsymbol{D}\mathcal{E}$ (in practice, one usually does not know what $\boldsymbol{D}\mathcal{E}$ is, although one might sense how big it is), a large reduction in control authority is demanded from methods like $\mathcal{H}_\infty$ to ensure robustness. This is due to the dependence of the modal input and output matrices, $\mathcal{E}^T\mathcal{B}$ and $\mathcal{C}\mathcal{E}$ on the mode-shape matrix. The problem with $\boldsymbol{D}\mathcal{E}$ illustrates the limitation associated with additive and multiplicative uncertainty models: The trade between robustness and performance can be severe for ML structures.

An improvement in the uncertainty model is possible, recognizing that it is the span of the columns of $\mathcal{E}$ that matters, not just the columns themselves. Nominal mode shapes span the same space as perturbed mode shapes provided the dynamics of the system are truncated properly. In models of the structure, it is not only necessary to retain the most significant modes of vibration, but also to ensure that all modes possessing similar substructural deformations are kept together.

In general, the number of modes retained for control design should be large enough to capture the significant dynamics of the system. If the number must be smaller than this, or if reduced models must be used, additive uncertainty must be used to capture the higher-order neglected dynamics. This introduces extra conservatism depending on how significant the neglected dynamics are.

If the mode shapes of the perturbed (actual) system are written in terms of the mode shapes of the nominal (modeled) system,

$$\mathcal{E}_p = \mathcal{E}\boldsymbol{N}_p \tag{8}$$

where $\boldsymbol{N}_p$ is a square, nonsingular matrix. The state transformation

$$\begin{bmatrix}\eta_p\\ \dot{\eta}_p\end{bmatrix} = \begin{bmatrix}\boldsymbol{N}_p^{-1} & \mathbf{0}\\ \mathbf{0} & \boldsymbol{N}_p^{-1}\end{bmatrix}\begin{bmatrix}\eta\\ \dot{\eta}\end{bmatrix} \tag{9}$$

when applied to Eqs. (5) and (6), yields

$$\begin{bmatrix}\dot{\eta}\\ \ddot{\eta}\end{bmatrix} = \begin{bmatrix}\mathbf{0} & \mathbf{1}\\ -\boldsymbol{N}_p\boldsymbol{\Omega}_p^2\boldsymbol{N}_p^{-1} & -2\boldsymbol{N}_p\boldsymbol{\Psi}_p\boldsymbol{N}_p^{-1}\end{bmatrix}\begin{bmatrix}\eta\\ \dot{\eta}\end{bmatrix} + \begin{bmatrix}\mathbf{0}\\ \boldsymbol{N}_p\boldsymbol{N}_p^T\mathcal{E}^T\mathcal{B}\end{bmatrix}f \tag{10}$$

$$\boldsymbol{y} = [\mathcal{C}\mathcal{E}\quad \mathbf{0}]\begin{bmatrix}\eta\\ \dot{\eta}\end{bmatrix} \tag{11}$$

Now the real perturbations can be rewritten as

$$\Delta\mathcal{E}^T = (\boldsymbol{N}_p\boldsymbol{N}_p^T - \mathbf{1})\mathcal{E}^T \tag{12}$$

$$\Delta\boldsymbol{\Omega}^2 = \boldsymbol{N}_p\boldsymbol{\Omega}_p^2\boldsymbol{N}_p^{-1} - \boldsymbol{\Omega}^2 \tag{13}$$

$$\Delta\boldsymbol{\Psi} = \boldsymbol{N}_p\boldsymbol{\Psi}_p\boldsymbol{N}_p^{-1} - \boldsymbol{\Psi} \tag{14}$$

When mass errors are zero (mass properties can in principle be measured with great accuracy) both the nominal and perturbed mode-shape matrices normalize the mass matrix, and the transformation $\boldsymbol{N}_p$ is orthonormal. This results in a new mode-shape perturbation that is zero, within numerical error. In practice, mass properties are easily measurable and tend to be more certain than stiffness and damping properties. As a result, one expects $\Delta\mathcal{E}$ to always possess a relatively small norm in comparison to the norm of $\mathcal{E}$

This analysis implies that mode-shape errors can be mostly eliminated if the perturbations to the natural frequency and damping matrices are not restricted to diagonal matrices. This is the justification behind using eigenvalue perturbations as the principle sources of uncertainty by Smith et al.[15] and Balas and Young.[16]

Structured uncertainty, like diagonal matrix uncertainty, for example, allows reductions in overconservatism because more information about the system is available. In cases where ML is a problem, however, there is a trade between keeping diagonal uncertainties diagonal versus eliminating the generally large unstructured uncertainty associated with the mode-shape matrix. In the experience of the authors, the latter is of much greater importance because it directly impinges on the resulting control authority. The norm of the mode-shape perturbation is directly proportional to the weight on the control forces.

Smith[14] has shown that the eigenvalues of $\boldsymbol{\Lambda}+\boldsymbol{W}\boldsymbol{\Delta}$ lie in the union of disks centered at the eigenvalues of $\boldsymbol{\Lambda}$ whose radii are defined by the elements of the real diagonal matrix $\boldsymbol{W}$. Here $\boldsymbol{\Lambda}$ is a diagonal matrix, and $\boldsymbol{\Delta}$ is a complex matrix whose norm is bounded by unity. Smith also extends this result to diagonalizable $\boldsymbol{A}$ matrices found in state-space plant representations and to real $\boldsymbol{\Delta}$. The

uncertainty model effectively defines disks around the poles of the system. When Λ is known always to be real, the use of a complex Δ leads to nonphysical eigenvalues that cannot occur in the actual system. This introduces some conservatism. For FSS, however, this conservatism is outweighed by overly conservative representations of mode-shape uncertainty through unstructured perturbation matrices. It can also be shown that complex (nonphysical) natural frequency perturbations have an interpretation in terms of changes in frequency and damping.

By using a similar form for the problem at hand, the perturbed modal matrices in Eq. (10) can be represented as follows:

$$N_p N_p^T \mathcal{E}^T \longrightarrow \mathcal{E}^T + \Delta_{\mathcal{E}^T} W_{\mathcal{E}^T} \tag{15}$$

$$N_p \Omega_p^2 N_p^{-1} \longrightarrow \Omega^2 + \Delta_{\Omega^2} W_{\Omega^2} \tag{16}$$

$$N_p \Psi_p N_p^{-1} \longrightarrow \Psi + \Delta_{\Psi} W_{\Psi} \tag{17}$$

where $\Delta_{\mathcal{E}^T}$, Δ_{Ω^2}, and Δ_{Ψ} are unknown, norm-bounded matrices. If the norm bounds are unity, the elements of W_{Ω^2} and W_{Ψ} define the radii of uncertainty around squared natural frequencies and damping factors in the complex plane. Because mass errors are generally small, $W_{\mathcal{E}^T}$ can be assumed to be negligible or near zero. (Note that the certainty of mass properties in comparison to stiffness and damping properties depends on the accuracy of measurement and varies on a case by case basis).

If the input matrix $\mathcal{B}$ is uncertain, however, because of potential errors in actuator gains and/or alignment, the weight $W_{\mathcal{E}^T}$ can be used to capture this information. Sensor uncertainty can also be approximately handled in this way (see Boulet et al.[17]).

Uncertainty weights can be generated systematically by constructing a set of representative $\mathcal{E}_p$ based on the control designer's knowledge of the coupling strength in the system, the expected levels of physical imperfection, and how the quotient of these two things can be translated into the degree of ML in the system. Because there are no closed-form solutions relating this quotient to ML, numerical analyses must be relied upon to gain an understanding of this relationship. In general, adjusting the parameters in a finite element model gives the needed information. Because manipulating a finite element model can be computationally intensive, this could be done only once to get an idea of the severity of ML. Other representative $\mathcal{E}_p$ could be coarsely estimated based on this (it is not important that they be entirely accurate, just that they be qualitatively similar, of full column rank, and span the same column space as $\mathcal{E}$). The representative $\mathcal{E}_p$ can then be used to generate the uncertainty weights via Eqs. (8) and (15–17). This is also an iterative process because one does not generally know what the actual perturbations are (otherwise the model would not be uncertain). Other approaches are summarized by Zee.[12]

The uncertainty model is now assembled into a simple formulation for $\mathcal{H}_\infty$ control. Again, the objective is to demonstrate the value of eigenvalue perturbation concepts through experiments on the ML-afflicted Daisy facility.

Formulating an Illustrative Control Problem

The diagram for robust control is shown in Fig. 3. For convenience, the uncertainties, input channels, and output channels are grouped together as follows:

$$\Delta = [\Delta_{\mathcal{E}^T} \quad \Delta_{\Omega^2} \quad \Delta_{\Psi}] \tag{18}$$

$$w_n = \mathrm{col}\{w_1, w_2\} \qquad z_n = \mathrm{col}\{z_1, z_2\} \qquad z_p = \mathrm{col}\{z_{\mathcal{E}^T}, z_{\Omega^2}, z_{\Psi}\} \tag{19}$$

The goal of robust $\mathcal{H}_\infty$ control is to minimize the $\mathcal{H}_\infty$ norm (maximum system gain over all frequencies) between the exogenous inputs w and controlled outputs z. These quantities are defined as

$$w = \mathrm{col}\{w_p, w_n\} \qquad z = \mathrm{col}\{z_p, z_n\} \tag{20}$$

to maintain stability and performance in the presence of uncertainty. When the $\mathcal{H}_\infty$ norm between w and z is optimized below unity by a suitable choice of controller K, the performance gain between w_n and z_n is guaranteed for all perturbations Δ of norm less than one.

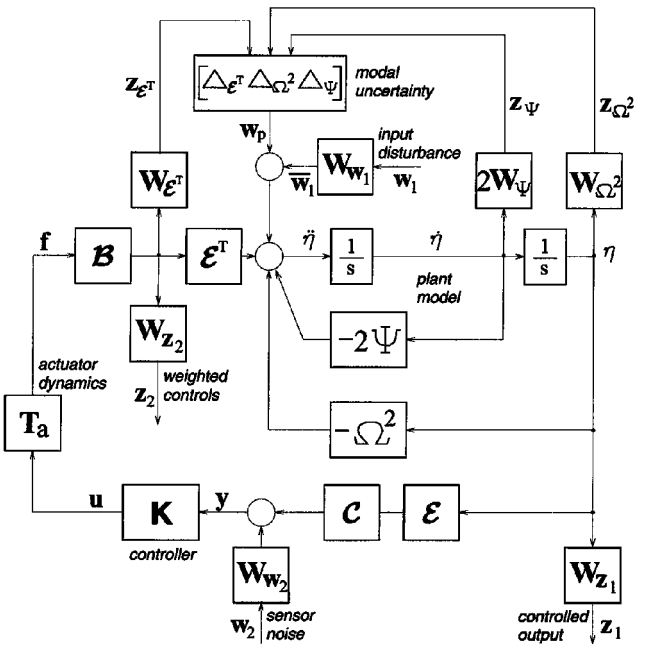

Fig. 3 Robust control diagram using eigenvalue perturbations.

Control design can be made easier in this case by setting $z = z_p$, if W_{Ω^2} and $W_{\mathcal{E}^T}$ assimilate W_{z_1} and W_{z_2}, respectively. The adjacency of W_{Ω^2} and W_{z_1} illustrates that eigenvalue perturbation models have the effect of aligning performance and robustness goals. Moreover, the gross reduction of $W_{\mathcal{E}^T}$ prevents mode-shape errors from swamping the control force weights W_{z_2} and eliminates any unnecessary restriction on control authority.

Synthesis of Controllers for Daisy

To begin Daisy's treatment for a rather severe case of ML, the preceding formulation is applied using a perfectly symmetric model of the structure. The challenge in controlling ML-afflicted structures lies in using limited actuation and/or sensing schemes. With Daisy's hub locked in place, the control objective for this study is to regulate the ribs to their conical resting configuration without using the in-cone thrusters of ribs 2, 5, 7, and 10. All 20 rib angles are measured. This is referred to as limited shape control in that a limited number of actuators are used to control the shape of the cone formed by the ribs. Despite the rib thrusters being very nonlinear devices, they are approximated as ideal torque devices for control design (no actuator dynamics are assumed).

A full-order Daisy model is used for control design, although a full-order model in the case of Daisy's discrete flexibility can be conceptualized as a reduced model of a FSS with continuous flexibility, truncated to the most significant modes of interest. In general, one rarely knows the exact characteristics of the system. For this reason, this same model is used in simulation.

Although out-of-cone modes are affected the most by ML, coupling between ribs in the out-of-cone direction is so weak that controllability is a problem without using all out-of-cone actuators. This does not mean that control is not possible, but that vibration suppression using a limited number of out-of-cone thrusters would require very long settling times, exceeding the data collection capabilities of Daisy. That is why an actuation scheme involving a reduced set of out-of-cone thrusters is not considered here. The reduced controllability and observability associated with limited control and weak coupling do not invalidate the usefulness of eigenvalue perturbation models for controlling systems afflicted with ML. The goal of this study is to demonstrate effective control when actuation is limited, ML is present, and sufficient controllability exists. This is possible by focusing on the in-cone modes alone.

From Table 2, one might select the in-cone thruster of Rib 6 as ideal for elimination, given that the first in-cone mode localizes strongly to that rib. However, Hong[13] has shown that intrarib coupling (unmodeled coupling between the out-of-cone and in-cone directions) is so severe in Rib 6 that vibrations would propagate quickly to the out-of-cone direction and be damped by the out-of-cone thruster. By qualitatively looking at empirically measured mode shapes and comparing length scales in Table 2, Ribs 2, 5, 7, and 10 are good choices for reduced actuation.

With the chosen actuation and sensing scheme, two control design strategies are available based on the scope of the resulting controllers, each resulting in a 20 input and 16 output controller.

1) With the decentralized strategy a separate controller is designed for each rib using only the thrusters for that rib. Because all ribs are assumed to be identical for control design, the same controller can be used for each (minus the in-cone control forces for Ribs 2, 5, 7, and 10). For this strategy, rib coupling is ignored because coupling is weak. Vibrations in the unactuated coordinates are expected to propagate to actuated ribs based on the assumption of perfect symmetry. (A controller of order 32 is achieved with this strategy).

2) With the centralized strategy a single controller is designed for the structure using all available thrusters. (A controller of order 40 is achieved with this strategy).

In most cases, breaking up the system into smaller physical portions makes the problem more manageable. A centralized controller can be designed for each portion. In the decentralized strategy, however, the decomposition is intentionally carried too far, to the point of relying on energy propagation for performance. For ML-afflicted structures, this reliance will, in fact, lead to poor performance because disturbance energy will tend to remain confined to local portions of the structure.

In general applications, control design weights are usually assigned to maximize robustness while maintaining desired performance levels. Uncertainty sizing is actually an iterative process because one does not know a priori how far off the structural model is from reality. The iterative process of implicitly sizing uncertainty is largely dependent on achieved laboratory performance; that is why experiments are important in determining proper error bounds.

In this demonstrative study of Daisy, however, uncertainty bounds are not determined based on empirical estimates, but on the maximum limits achievable while maintaining predicted closed-loop stability (remarkably, as explained further on, this does not hamper achievable performance). Although empirically observed properties are available, they will only be used to understand the results and the ultimately achieved performance. In practice, empirical information may not be available, and so will not be relied on for control design here. The nominal model of Daisy used for analysis and control design is based on ideal mass and stiffness properties yielding the ideal frequencies shown in Table 2. Damping ratios for all nominal modes are assumed to be 2%. In lieu of experimental uncertainty sizing, Monte Carlo simulations are used to generate random models perturbed by predefined amounts in mass, stiffness, and damping from the nominal model. The perturbations in modal coordinates are calculated for each perturbed model, and the norms of the matrices defined in Eqs. (12–14) are determined. These norms form three sample spaces, each with 1000 samples. The constant weights $\boldsymbol{W}_{\mathcal{E}^T}$, $\boldsymbol{W}_{\Omega^2}$, and $\boldsymbol{W}_{\Psi}$ are defined as the average norm plus three standard deviations over each sample space, respectively, multiplied by the identity matrix. Table 3 summarizes the constants used to define the weights $\boldsymbol{W}_{\mathcal{E}^T}$, $\boldsymbol{W}_{\Omega^2}$, and $\boldsymbol{W}_{\Psi}$ when multiplied by the identity matrix for each design approach. In the decentralized case, separate out-of-cone and in-cone analyses are conducted for a representative rib model.

Table 3 Uncertainty weights

$\boldsymbol{W}_{\mathcal{E}^T}$	$\boldsymbol{W}_{\Omega^2}$	$\boldsymbol{W}_{\Psi}$
	Decentralized	
0.087 (OC)	0.120 (OC)	0.005 (OC)
0.088 (IC)	0.225 (IC)	0.006 (IC)
	Centralized	
0.026	0.034	0.001

For decentralized design, a maximum predicted tolerance of 10% in mass, stiffness, and damping properties is achieved. This corresponds to the weights shown in Table 3 and is based on iteratively designing preliminary controllers using the formulation in Fig. 3, where the performance weights $\boldsymbol{W}_{z_1}$, $\boldsymbol{W}_{z_2}$, $\boldsymbol{W}_{w_1}$, and $\boldsymbol{W}_{w_2}$ are chosen to be zero or as close to zero as possible while still regularizing the $\mathcal{H}_\infty$ problem. At each iteration, the controller together with the plant model are analyzed for closed-loop stability. The maximum achievable uncertainty levels are defined by the largest uncertainty weights allowed before instability ensues. Similarly, a maximum predicted tolerance of 2.5% in mass, stiffness, and damping properties is achieved for the centralized design case.

After determining uncertainty weights for this demonstrative study using the described procedure, controllers are designed using the nominal, ideal Daisy model. To regulate the ribs to their conical resting configuration, the performance objective becomes one of driving η to zero. The weight $\boldsymbol{W}_{z_1}$ is used for this purpose. This weight can be defined so that it translates coordinates from modal to physical space before weighting them if it is desirable to control physical coordinates directly. For this study, weighting the modal coordinates is sufficient. The individual elements of this constant, diagonal matrix are manipulated by trial and error to reduce the settling time of the ribs as much as possible. To reduce the number of outputs in the control design, the weights $\boldsymbol{W}_{z_1}$ and $\boldsymbol{W}_{\Omega^2}$ can be combined into one matrix, whose entries are the maximum of the entries in $\boldsymbol{W}_{z_1}$ and $\boldsymbol{W}_{\Omega^2}$. If the matrices were not constant, the combination would involve defining the maximum entries at each frequency.

The weight $\boldsymbol{W}_{z_2}$ is used to limit control force authority and bandwidth to avoid actuator saturation and to provide gain stability. This matrix can also be combined with $\boldsymbol{W}_{\mathcal{E}^T}$ to reduce the number of outputs. The weights $\boldsymbol{W}_{w_1}$ and $\boldsymbol{W}_{w_2}$ are used for sizing input disturbances and sensor noise, respectively. The sensor noise weighting can also be used to limit the bandwidth of the controller. These weights are jointly determined by trial and error along with $\boldsymbol{W}_{z_1}$ to minimize rib settling time. Weight selection is an iterative process involving control design and verification via simulation. Larger entries in $\boldsymbol{W}_{z_1}$ and $\boldsymbol{W}_{w_1}$ increase the disturbance rejection capabilities of the controller, increasing gain and bandwidth and reducing settling time. Increasing $\boldsymbol{W}_{z_2}$ and $\boldsymbol{W}_{w_2}$ has the effect of limiting gain and bandwidth to improve overall stability, but at the cost of longer settling times.

Constant, diagonal weights are sufficient for this study because the dynamics of Daisy are slow compared to the target sample frequency of 10 Hz (controllers are designed in continuous time and then discretized). In the simulations and experiments that follow, frequencies above 1 Hz are never excited, avoiding aliasing concerns and the need for frequency-dependent weighting functions. Although the presented formulation does permit frequency-dependent weights, which are especially useful for cases involving truncated dynamics, they are not essential to the current analysis of Daisy.

The final entries along the main diagonal of each weighting matrix are summarized in Table 4. Where single numbers are shown, a multiplication by the identity matrix is implied. In some cases, the out-of-cone (OC) and in-cone (IC) coordinates are weighted differently for each rib. These are indicated by OC, IC, and rib numbers. Where no rib numbers are specified, the entire set of OC or IC coordinates is implied.

As a result of combining weighting matrices, for example $\boldsymbol{W}_{z_1}$ and $\boldsymbol{W}_{\Omega^2}$, a duality in the performance and robustness objectives

Table 4 Control performance weights

$\boldsymbol{W}_{z_1}$	$\boldsymbol{W}_{z_2}$	$\boldsymbol{W}_{w_1}$	$\boldsymbol{W}_{w_2}$
	Decentralized		
0.20 (OC)	0.18	1	0.6
0.24 (IC)			
	Centralized		
0.17 (OC)	0.05 (OC)	0.9 (OC)	0.6 (OC)
0.065 (IC: 1–3, 5, 7–10)	0.04 (IC)	0.3 (IC)	0.1 (IC)
0.06 (IC: 4, 6)			

is apparent. The combination aligns performance and robustness goals, and so an assurance is always provided that performance or robustness objectives will be met or exceeded. In other words, what is good for performance is good for robustness and vice versa in this case. By maximizing robustness, performance is also maximized. The choice of the 10% and 2.5% uncertainty limits, therefore, does not hamper, but improves the achievable performance determined by the entries in $\boldsymbol{W}_{z_1}$.

The resulting controllers yield closed-loop $\mathcal{H}_\infty$ norms of 0.979 (decentralized, for each rib) and 0.984 (centralized), thus, guaranteeing robust stability and robust performance. That is, the norms between $\boldsymbol{w}_n$ and $\boldsymbol{z}_n$ (performance) and between $\boldsymbol{w}_p$ and $\boldsymbol{z}_p$ (stability) are guaranteed to be less than unity simultaneously even in the presence of uncertainty.

To deduce the guaranteed stability ranges imparted by the modal uncertainty weights in Table 3 for the decentralized rib case, note that the squared natural frequencies of a rib are nominally 0.330 s^{-2} and 0.535 s^{-2} for the OC and IC directions respectively. Damping factors are correspondingly 0.017 s^{-1} and 0.022 s^{-1}. By applying the results of Smith,[14] we see uncertainty limits of ±0.2 and ±0.24 (see Table 3) exist on the OC and IC squared frequencies for the decentralized design case (noting that the maximum tolerable norm on Δ_{Ω^2} is close to unity since this is the dominant uncertainty in Δ). These limits are about 45 and 60% of the nominal squared frequencies. Similar application of Smith's results to the centralized design indicates limits of approximately 10% in squared natural frequency. Damping uncertainty weights range from 6% (centralized design) to 30% (decentralized design) of the nominal rib damping factors. Because, damping is very weak (2% nominal damping ratio for all modes), however, its uncertainty contributes minimally to Δ and does not have a major impact on control design.

Interestingly, the mode-shape uncertainty weights are always small and never rival the $\boldsymbol{W}_{z_2}$ control force weights used to prevent actuator saturation. This is in keeping with what was said earlier; that is, control authority is not overly restricted by mode-shape uncertainty when using eigenvalue perturbation models.

Results

The controllers designed for Daisy are analyzed through simulations. The following tests are performed for both the decentralized and centralized controller designs.

1) For nominal performance, the controller and the nominal, ideal (i.e., all ribs the same) plant model are subjected to separate initial 1.75-s pulse inputs of 0.36 Nm at the tip of each rib in both the OC and IC (except for ribs 2, 5, 7, and 10) directions. The initial conditions are zero. Performance is determined by settling time or the time for all ribs to reach 10% of their maximum deflections. The results for each pulse input simulation are used to determine an overall worst-case settling time.

2) For robust stability, the controller and increasingly perturbed plant models are subjected to the pulse disturbances described earlier. Perturbed plant models are defined based on randomly generated mass, stiffness, and damping matrices within predefined limits in structural properties. Five perturbed plant models are generated for each of the following cases: 5, 10, 15, 20, 30, and 40% variations in mass, stiffness, and damping properties. These cases correspond roughly to 10, 20, 30, 45, 70, and 90% variations in squared natural frequencies. The robust stability level is defined as the largest tested variation level for which the closed-loop system remains stable.

3) For robust performance, the controller and increasingly perturbed plant models are subjected to the pulse disturbances described earlier. Perturbed plant models are the same as those used for the robust stability tests. The robust performance level is defined as the largest tested variation level for which the worst-case settling time is within 10% of the nominal worst-case settling time (as defined for nominal performance).

In simulation, maximum rib deflections resulting from the pulse disturbances range from 5 to 6 deg. The decentralized design yields a nominal worst-case settling time of 100 s. Marginal instability occurs for 40% variations in mass, stiffness, and damping properties but the closed-loop system remains stable for 30% variations in these properties. The robust performance level, for a worst-case settling time of under 110 s, is obtained for 10% variations in mass, stiffness, and damping properties but not for 15% variations. Variations of 15% or higher induce ML in the IC modes of the structure. Although the analytical results predict robust performance up to 25% variations in physical properties (45–60% variations in squared natural frequencies), the actual robust performance level achieved is far less because of the inability of disturbance energy to propagate to well-actuated regions of the structure. Once modes localize, the worst-case settling times approach those of the open-loop system (where only natural damping removes energy from the system), at around 3 min.

For the centralized design, the nominal worst-case settling time is 40 s, illustrating the benefits of centralization. Robust stability is demonstrated for variations in mass, stiffness, and damping properties up to 30% of nominal properties. Robust performance (settling times of 44 s or under) is demonstrated for variations in physical properties up to 20%. This exceeds the analytical predictions of the last section (5% variations in physical properties, or 10% variations in squared natural frequency) and shows that performance is maintained even after modes localize and free vibrations fail to propagate from one rib to the next. The centralized control design not only demonstrates the benefits of centralization, but also the value of eigenvalue perturbation models in the presence of ML.

As a final result, the authors present one more test to compare simulations against laboratory experiments. Again, the controllers designed for Daisy are evaluated by observing the vibration suppression performance after an initial disturbance is injected into the system. A square pulse disturbance of 0.36 Nm is applied for 1.75 s in the positive OC and IC directions for ribs 1–5 and in the negative directions for Ribs 6–10. The disturbance profile is chosen to excite all modes while observing the limitations of the rib sensors. As a result of the disturbance, all ribs have an initial deflection of about 6 deg. Rib 7 is a representative candidate for showing results graphically, along with its neighbors, Ribs 6 and 8. Rib 7 has the slowest decay under control. Results for all ribs are presented by Zee,[12] and demonstrate as good or better decay responses. Graphical presentation of all ribs is not possible here due to space limitations. The IC performance of Ribs 2, 5, and 10 is comparable to that of Rib 7, and the OC decay is very good for each controller.

In the decentralized case, OC settling times are under 5 s. The IC settling times for each rib are comparable to the OC times when the rib's IC coordinate is actuated. When not actuated, the IC settling times are considerably longer. Figure 4 illustrates 1) the experimental open-loop IC response of Rib 7, 2) the simulated IC response of Rib 7 when the controller is applied to the nominal plant model with uniform and ideal rib properties (the model used for control design), 3) the experimental IC response of Rib 7 when the controller is applied to Daisy, 4) the experimental IC response of Rib 6 when the controller is applied to Daisy, and 5) the experimental IC response of Rib 8 when the controller is applied to Daisy.

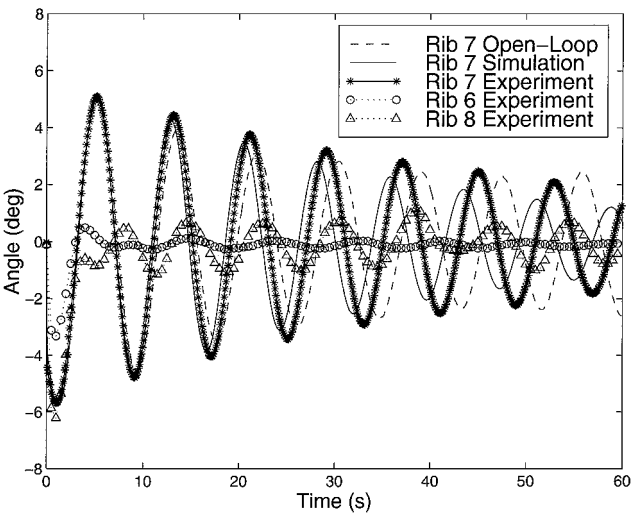

Fig. 4 IC response of rib 7, decentralized design.

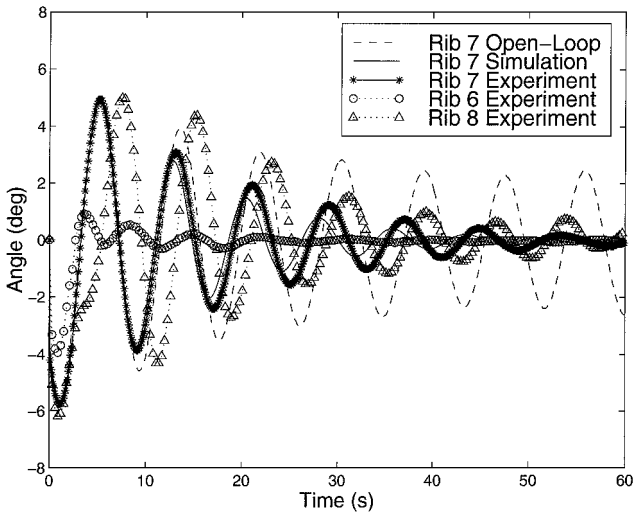

Fig. 5 IC response of rib 7, centralized design.

As indicated from Table 2, through empirical observation, the modes of the actual structure are localized. Table 1 shows that the errors in natural frequency range from 1 to 26% of nominal (which translates to under 60% variations in squared natural frequency). According to the analytical predictions of the preceding section, robust performance should be guaranteed for these errors. Unfortunately, because modes are localized, the experimental closed-loop response of Rib 7 indicates a settling time noticeably higher than that predicted through simulating the nominal plant. In fact, the experimental settling rate is comparable to the open-loop response. Simulation overpredicts the decay rate because it uses a plant model that assumes perfect structural symmetry. The localization of modes, especially Mode 15 to Rib 7 (see Table 2), has reduced the ability of vibrations to propagate freely from one rib to the next. As a consequence, disturbance energy is not absorbed effectively by neighboring ribs. Here neighboring ribs are effective at removing their own vibrations, but have difficulty in removing energy from Rib 7. This difficulty is not only due to weak coupling between ribs, but also is aggravated by ML.

OC settling times for the centralized design are under 10 s. The IC performance for all ribs is qualitatively similar to that of Rib 7. Figure 5 shows the centralized controller, similar to those presented for the decentralized controller. When the ideal plant model is used in simulation, the closed-loop IC response of Rib 7 exhibits a settling time of around 40 s. The settling time for the experimental IC response of Rib 7 increases to only 44 s, illustrating the robust performance characteristics of the controller. In Fig. 5, the experimental in-cone responses of Ribs 6 and 8 show that the energy is truly dissipated and not sent to other parts of the structure. As indicated by Table 2 the modes of the actual structure are localized. The natural frequency errors are a maximum of 10% of the ideal natural frequencies (a variation of 20% in squared natural frequency). Even though these errors fall outside the robustness bounds guaranteed analytically in the preceding section, the experimental response of Rib 7 is remarkably close to that predicted by simulating the ideal plant model. The centralized controller has maintained performance in the presence of ML, and the uncertainty model used for design was successful at capturing the system errors without overconservatism. Moreover, the experimental results illustrate that effective, robust control is possible in ML-afflicted structures.

Conclusion

The inability of free vibrations to propagate and the modeling uncertainty created by the ML phenomenon can cause problems for the high-performance control of flexible space structures comprising weakly coupled repeating members. Decentralized control is not effective for mode-localized structures with limited actuation and/or sensing because it relies on the propagation of energy through channels of weak coupling. The fulfillment of the requirement that free vibrations propagate is inhibited when modes localize. Centralized control is necessary to actively use intermember coupling to an advantage. However, ML also produces large model errors, especially in mode shapes, that may lead to reduced control authority and overconservative controllers.

Eigenvalue perturbation models are ideally suited for control design when a structure exhibits ML. Shifting errors from mode shapes to eigenvalues allows higher control authority, less overconservatism, and better performance. It has been demonstrated that a mode-localized structure can be controlled effectively through experiments performed on an FSS emulator. General insights and concrete suggestions have been offered to design controllers for flexible spacecraft with localized modes.

Acknowledgments

This research was supported by the Natural Sciences and Engineering Research Council of Canada. The first author is grateful to the Natural Sciences and Engineering Research Council of Canada for a full graduate fellowship during the period of investigation.

References

[1]Anderson, P. W., "Absence of Diffusion in Certain Random Lattices," *Physical Review*, Vol. 109, 1958, pp. 1492–1505.

[2]Cornwell, P. J., and Bendiksen, O. O., "A Numerical Study of Vibration Localization in Disordered Cyclic Structures," *30th AIAA/ASME/ASCE/AHS/ASC Structures, Structural Dynamics, and Materials Conference*, AIAA, Washington, DC, 1989, pp. 199–208.

[3]Chau, B. C. T., "A Perturbation Study of the Phenomenon of Mode Localization," M.A. Sc. Thesis, Inst. for Aerospace Studies, Univ. of Toronto, Toronto, ON, Canada, 1990.

[4]Kissel, G. J., "Localization in Disordered Periodic Structures," Ph.D. Thesis, Massachusetts Inst. of Technology, Cambridge, MA, 1988.

[5]Luo, W., and Wang, H., "Modal Analysis for Disordered Periodic or Nearly Periodic Structures," *Proceedings of the Tenth International Modal Analysis Conference*, Vol. 1, Society for Experimental Mechanics, Inc., Bethel, CT, 1992, pp. 606–611.

[6]Mester, S. S., and Benaroya, H., "Localization in Near Periodic Structures," *Proceedings of the 35th AIAA/ASME/ASCE/AHS/ASC Structures, Structural Dynamics, and Materials Conference*, AIAA, Washington, DC, 1994, pp. 1488–1496.

[7]Bendiksen, O. O., "Mode Localization Phenomena in Large Space Structures," *Proceedings of the 27th AIAA/ASME/ASCE/AHS/ASC Structures, Structural Dynamics, and Materials Conference*, AIAA, Washington, DC, 1986, pp. 325–335.

[8]Cornwell, P. J., and Bendiksen, O. O., "Localization of Vibrations in Large Space Reflectors," *Proceedings of the 28th AIAA/ASME/ASCE/AHS/ASC Structures, Structural Dynamics, and Materials Conference*, AIAA, Washington, DC, 1987, pp. 925–935.

[9]Levine-West, M. B., and Salama, M. A., "Mode Localization Experiments on a Ribbed Antenna," *AIAA Journal*, Vol. 31, No. 10, 1993, pp. 1929–1937.

[10]Shelley, F. J., and Clark, W. W., "Closed-Loop Mode Localization for Vibration Control in Flexible Structures," *Proceedings of the 13th American Controls Conference*, American Automatic Control Council, Green Valley, AZ, 1994, pp. 1826–1830.

[11]Zee, R. E., Hughes, P. C., Carroll, K. A., and Vukovich, G., "On-Orbit Dynamics, Identification and Control Experiments for Space Station Risk Mitigation," *10th Conference on Astronautics*, Canadian Aeronautics and Space Inst., Ottawa, 1998, pp. 45–49.

[12]Zee, R. E., "Control of Flexible Space Structures with Localized Modes," Ph.D. Thesis, Inst. for Aerospace Studies, Univ. of Toronto, Toronto, June 1997.

[13]Hong, T., "Time Delayed Control of Flexible Space Structures," Ph.D. Thesis, Inst. for Aerospace Studies, Univ. of Toronto, Toronto, June 1998.

[14]Smith, R. S., "Eigenvalue Perturbation Models for Robust Control," *IEEE Transactions on Automatic Control*, Vol. 40, No. 6, 1995, pp. 1063–1066.

[15]Smith, R. S., Chu, C. C., and Fanson, J. L., "The Design of H-Infinity Controllers for an Experimental Non-Collocated Flexible Structure Problem," *IEEE Transactions on Control Systems Technology*, Vol. 2, No. 2, 1994, pp. 101–109.

[16]Balas, G. J., and Young, P. M., "Control Design for Variations in Structural Natural Frequencies," *Journal of Guidance, Control, and Dynamics*, Vol. 18, No. 2, 1995, pp. 325–332.

[17]Boulet, B., Francis, B. A., Hughes, P. C., and Hong, T., "Uncertainty Modeling and Experiments in H-Infinity Control of Large Flexible Space Structures," *IEEE Conference on Control Applications*, Inst. of Electrical and Electronics Engineers, New York, 1995, pp. 1078–1085.